


Force reduction factor for out-of-plane simple mechanisms of masonry structures

Simona Coccia¹  · Fabio Di Carlo¹ · Stefania Imperatore²

Received: 11 November 2015 / Accepted: 26 July 2016 / Published online: 6 August 2016
© Springer Science+Business Media Dordrecht 2016

Abstract The dynamic behaviour of existing masonry buildings mainly depends on the out-of-plane response of the vertical walls. A proper evaluation of their response can be analytically performed considering the dynamic equation of motion of the rigid body, in the framework of rigid in compression no tension material. The above equation is numerically solved with increasing magnitude of the seismic action, until the collapse condition of the wall, due to a lack of equilibrium, is reached. In the paper two local collapse mechanisms are considered, the two sided and the one sided rocking. The influence of considering a simplified trilinear moment-rotation law is also discussed. For each mechanism, the force-reduction factor, defined as the ratio between the seismic acceleration value causing the collapse of the masonry element and the one corresponding to the activation of the rocking motion, is evaluated. The dependence of this factor on the main parameters of the model is deeply investigated by means of numerical analyses, varying the geometrical characteristics of the panel, the energy dissipation model and the features of the seismic input. A power function law between an effective force reduction factor, defined as the ratio of the force reduction factor multiplied for the gravitational acceleration to the peak ground acceleration, and the Housner Spectrum Intensity is identified for both the examined models. These laws allow accounting for the so-called scale effect within a force-based framework. Eventually, novel formulations for evaluating the force reduction factor of two and one sided rocking systems are here proposed. Their effectiveness has been also highlighted considering both spectrum-compatible accelerograms and natural records.

Keywords Unreinforced masonry · Rocking · Force reduction factor · Local collapse mechanism

✉ Simona Coccia
coccia@ing.uniroma2.it

¹ Department of Civil Engineering and Computer Science Engineering, University of Rome “Tor Vergata”, Rome, Italy

² University “Niccolò Cusano”, Rome, Italy

1 Introduction

The problem of the seismic assessment and retrofit of existing unreinforced masonry buildings has become one of the main topics of interest in the world of constructions. Post-earthquake damage surveys and shaking table laboratory tests have shown that the main vulnerability of masonry structures with poor connections between orthogonal walls or walls and floors is associated to local failure modes, specifically related to the out-of-plane response (D'Ayala and Paganoni 2011). Assuming the hypothesis of rigid in compression and no tension material, the collapse load of masonry structures can be evaluated with two different approaches: an equivalent static method based on the Limit Analysis theory in the un-deformed configuration (D'Ayala et al. 1997; D'Ayala and Speranza 2003; Coccia et al. 2015a; Coccia and Como 2015) or in the deformed configuration (Coccia et al. 2015b) and a dynamic approach in the case of inertial horizontal actions. According to this last approach, each masonry pier or spandrel is schematized in a macro-element, modelled as a rigid body excited into a rocking motion upon a rigid horizontal base. Unilateral contacts, impacts and sliding with friction may occur at the interface sections of the macro-element, causing a kinetic energy dissipation. Therefore, the analysis of the dynamic problem of a rocking element acquires fundamental importance in order to define a realistic “seismic force reduction factor”, called *q-factor* in Europe and *R-factor* in the United States, which takes account of the ratio between non-linear dynamic response and static activation of motion. A complete assessment of this parameter, for a masonry element undergoing to an out-of-plane motion, is still missing. Further researches having the aim to investigate the main parameters affecting the rocking response are then required. The seismic behaviour of a single masonry wall depends on its position within the structure. Admitting that a simple overturning mechanism can develop, the considered macro-element may be subjected to two distinct kinematic mechanisms. The first, typical of isolated elements, is called in the following “two sided rocking” and it is characterised by a rocking motion along both the inward and outward directions. The second considered mechanism, called “one sided rocking”, is instead related to a masonry wall characterised by the presence of an element that avoids inward rotation (e.g. a slab, a diaphragm floor or a transverse wall). Other studies have been also developed in order to account for the effect of constraint from lateral walls at the corners of the buildings (D'Ayala and Shi 2011). Since in the present work the behaviour of historical masonry buildings characterized by poor connections with lateral or internal perpendicular walls is investigated, the latter effect is not considered.

In literature, analytical, experimental and numerical studies are available, but the definition of adequate force reduction factors is still missing. Experimental investigations are typically effected in order to calibrate either numerical and analytical models (Sorrentino et al. 2011; Costa et al. 2012). Numerical models are also based on the distinct element approach (DEM), and permit to simulate either the two sided and the one sided rocking mechanisms (Papantonopoulos et al. 2002; Peña et al. 2007; De Felice 2011). The effectiveness of the numerical response clearly depends on the imposed boundary condition, specifically those related to the energy dissipation phenomenon. The analytical models, finally, differ in the considered kinematic mechanism and consider steady state harmonic functions, simple pulses or natural and artificial spectrum-compatible acceleration time histories (Yim et al. 1980; Makris and Konstantinidis 2003; Sorrentino et al. 2008b; Shawa et al. 2012; Giresini et al. 2015).

The dynamic equation of the motion of the two sided rocking model was firstly developed by Housner (1963), who modelled the element as a rigid inverted pendulum

structure in absence of sliding between block and foundation. The overturning modes of a rigid block exhibiting one or more impacts were investigated by Zhang and Makris (2001), Kounadis (2010) and Hao and Zhou (2011). Prieto and Lourenço (2005) introduced a novel formulation for the rocking motion of a rigid block, based on a single ordinary differential equation, which also defined the damping effects by means of impulsive forces. The response of the block to different acceleration time histories has been widely treated by Sorrentino et al. (2006) and Sorrentino et al. (2008a).

The first analytical study of the one sided rocking model was developed by Hogan (1992), who analysed the dynamical problem of an inverted pendulum structure impacting on a side under harmonic forcing. Subsequently other authors, introducing the seismic input in the model, stated the importance of a correct assessment of the energy dissipation to properly evaluate the effective rocking behaviour of the masonry wall (Sorrentino et al. 2008a; Shawa et al. 2012). Due to this reason, the authors carried out experimental investigations in order to estimate the kinetic energy dissipated at impact.

In this paper, the dynamic response of the two considered local collapse mechanisms is investigated by means of numerical integrations of the equation of motion of the rigid block, in the framework of rigid in compression no tension material. The aim of the work is the definition of effective formulations for evaluating the force-reduction factor, defined as the ratio between the seismic acceleration value causing the collapse of the masonry element and the one corresponding to the activation of the rocking motion. The collapse condition is due to a lack of equilibrium and the development of cracking within the body is not here considered.

2 Equations of motion of the considered mechanisms

In the analytical model of the two sided rocking mechanism, the body deformability is neglected and the coefficient of friction is assumed to be sufficiently large to prevent horizontal sliding between the block and the rigid foundation (Housner 1963). The only possible motion is then the rotation about the outside edges of the block (points O and O' in Fig. 1).

The main geometrical properties of the model are the radial distance R (from the centre of mass G to each one of the two centres of rotation O and O') and the angle α between the line R and the side of the block, representing a measure of the slenderness of the block.

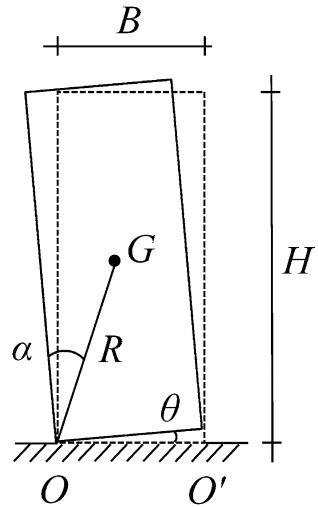
The equation of motion is obtained applying the Lagrange Equation to the block of Fig. 1:

$$\ddot{\theta} + p^2 \cdot \sin(\alpha - \theta) = p^2 \cdot \left[\frac{\ddot{u}(t)}{g} \cdot \cos(\alpha - \theta) \right] \quad (1)$$

where (\cdot) means differentiation with respect to time t , $\ddot{u}(t)$ is the time-dependent ground motion acceleration, g is the gravitational acceleration, m is the mass of the block, I_G is the moment of inertia about the centre of gravity, $p^2 = \frac{m \cdot g \cdot R}{I_0}$ is the frequency parameter of the block and $I_0 = I_G + m \cdot R^2$ is the moment of inertia about the two centres of rotation. The system is characterized by a threshold acceleration a_{RM} , defined as the acceleration value for which the moment due to self-weight equals the overturning moment due to seismic action:

$$a_{RM} = g \cdot \tan \alpha \quad (2)$$

Fig. 1 Model geometry



In this paper, only non-load carrying elements are considered, for which the overturning condition, corresponding to the failure of the block, consists in the attainment of a rotation higher than the slenderness angle α . During the forced oscillatory motion, the rotation of the block can exceed the angle α , because a consecutive contrary pulse can bring the system again in an equilibrium condition.

Whenever an impact occurs, dissipative phenomena take place, determining a damping in the oscillatory motion of the block. In the paper, these effects are modelled according to the classical approach based on the conservation of angular momentum with the hypotheses of infinitesimal duration of the impact, no displacement and instantaneous variation of velocity during impact (Housner 1963; De Lorenzis et al. 2007; Sorrentino et al. 2008a; Costa et al. 2012).

Housner (1963) introduced a relationship between the velocity of the block before ($\dot{\theta}_1$) and after ($\dot{\theta}_2$) the impact, depending on the parameter r (named coefficient of restitution), defined as the ratio between the kinetic energies before and after the impact:

$$\dot{\theta}_2 = \dot{\theta}_1 \cdot \sqrt{r} \tag{3}$$

The theoretical coefficient of restitution depends only on the geometry of the block and for the case of rectangular block becomes:

$$r = \left(1 - \frac{2bR \sin \alpha}{I_0}\right)^2 = \left(1 - \frac{3}{2} \sin^2 \alpha\right)^2 \tag{4}$$

where b is the half-width of the block.

Experimental tests performed on different types of masonry walls have however shown a discrepancy with the theoretical values. For example, Sorrentino et al. (2011), testing two different masonry typologies, made of tuff units and solid clay bricks respectively, propose this relationship:

$$\sqrt{r_{exp}} = 0.95 \cdot \sqrt{r} \tag{5}$$

where r_{exp} is the obtained experimental coefficient of restitution.

Experimental tests performed by Costa et al. (2013) on sack stone masonry give a range of $\sqrt{r_{exp}}$ variable between $0.95 \cdot \sqrt{r}$ and 0.98. The same authors propose to use a value included in this interval in the analysis of the rocking behaviour of walls similar to the tested ones and suggest that the effects of repetition may lead to the result of Eq. (5).

It is worth of interest to highlight the existence of a scale effect according to which the smaller of two geometrically similar blocks is less stable than the larger one (Housner 1963; Sorrentino et al. 2006).

In the one sided rocking mechanism only rotations around the center O are allowed (Fig. 1). When the block falls back into the vertical position impacting with the base, the centre of rotation remains in the point O and the block continues to rotate around this latter but in the opposite direction. Due to this reason, the motion of the block can start only if the seismic acceleration acts along the correct direction. The motion of the block is again described by Eq. (1), in which a new boundary condition on the sign of the rotation has to be introduced.

Hogan (1992) developed the first model of energy dissipation for this mechanism, assuming for the coefficient of restitution r Eq. (4). Based on the approach of the conservation of the angular momentum, Sorrentino et al. (2011) suggest evaluating the coefficient of restitution assuming that the three impacts occur in sequence: the first on the base, the second against the upper corner and the last one again on the base, after the inversion of the block motion. The energy dissipation model is shown in Fig. 2.

For a rectangular block, according to Sorrentino et al. (2011), it is possible to estimate the theoretical coefficient of restitution of the one sided rocking as:

$$r_{1s} = \left[\left(1 - \frac{3}{2} \sin^2 \alpha \right)^2 \left(1 - \frac{3}{2} \cos^2 \alpha \right) \right]^2 \tag{6}$$

According to the outcomes of an experimental campaign, the same authors propose also another formulation for the coefficient of restitution:

$$r_{1s,exp} = r_{1s} \left[1.18 - 0.473 \left(\frac{\dot{\theta}_1}{\dot{\theta}_r} \right)^2 \right]^2 \tag{7}$$

in which $\dot{\theta}_1$ is the velocity of the block before the impact and $\dot{\theta}_r$ is the overturning velocity, defined as:

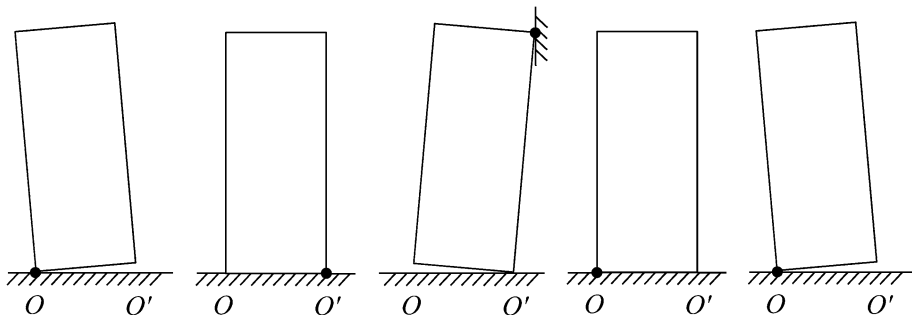


Fig. 2 Theoretical energy dissipation model for the one sided mechanism

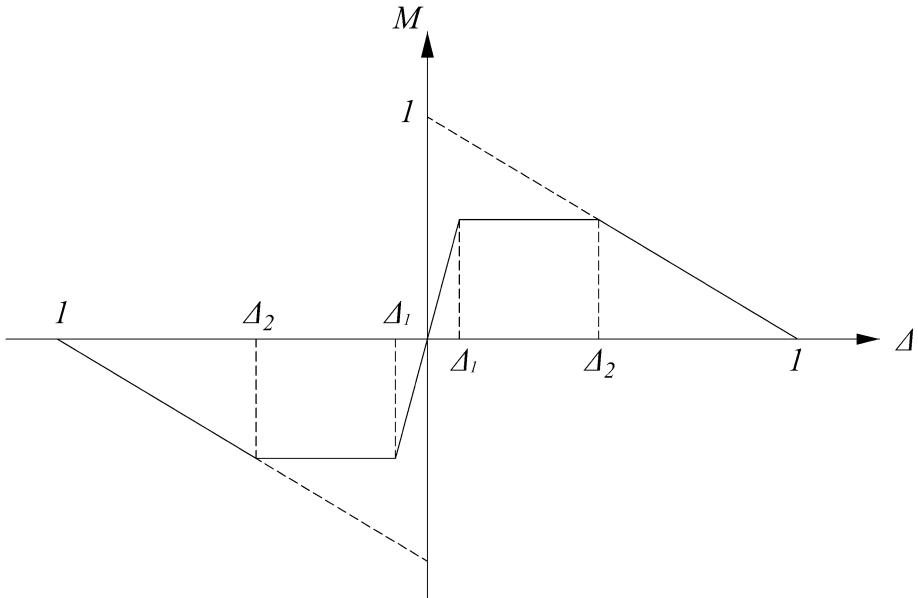


Fig. 3 Trilinear simplified moment-rotation law

$$\dot{\theta}_r = 2 \frac{mgR}{I_o} (1 - \cos \alpha) \tag{8}$$

The models previously described are defined considering a perfectly parallelepiped geometry of the wall. In order to account for a deviation of the actual geometry from the ideal one, the equation of motion can be modified considering a different moment-rotation law (Doherty et al. 2002; Sorrentino et al. 2008a; Al Shawa et al. 2015; Ferreira et al. 2015). This approach will be also used in the paper in a further section with the aim to highlight the differences with the classic theory. In particular, a simplified trilinear moment-rotation law with a finite initial stiffness is implemented, (Fig. 3). The three branches of the model are defined by means of two parameters, Δ_1 and Δ_2 , defined as the ratio between the angle of rotation and the slenderness angle of the block. The first parameter identifies the ending point of the initial elastic branch of the trilinear model while the second one defines the length of the steady part.

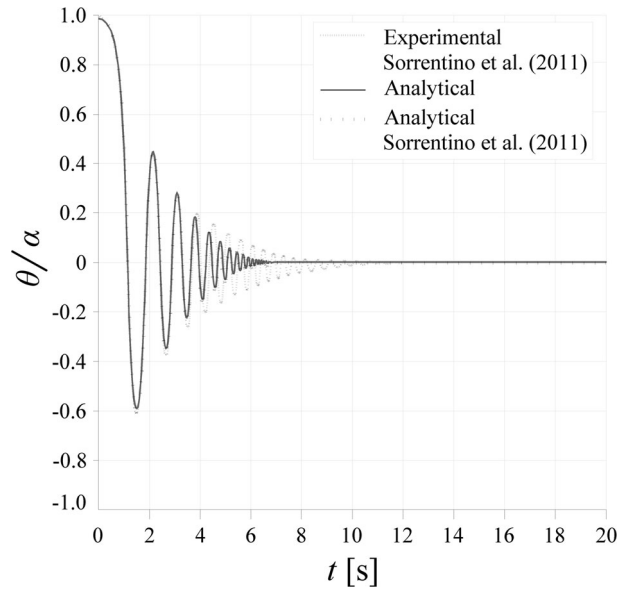
3 The force reduction factor

A simplified method to check the seismic safety of a masonry wall is proposed within the Italian Standard (CMIT 2009) and consists in the satisfaction of the inequality:

$$a_{RM} \geq \frac{S \cdot a_g}{q_{St}} \tag{9}$$

where a_{RM} is the threshold acceleration given by Eq. (2), $S \cdot a_g$ is the peak ground acceleration (PGA) and q_{St} is the force reduction factor given by the Code. According to the current approach presented in the Italian Standard, this latter is taken to be always equal

Fig. 4 Comparison between numerical and experimental free vibrations



to 2, regardless of the geometrical properties of the block, the type of mechanism and the seismic input. In order to evaluate the effective force reduction factor, incremental dynamic analyses are performed on masonry walls.

The equation of motion (Eq. 1), in which the seismic input $ii(t)$ is increased by means of a multiplier C , is numerically solved using the Newmark trapezoidal rule, until the overturning condition is reached (Coccia et al. 2016).

In order to demonstrate the effectiveness of the integration procedure in the modelling of the rocking behaviour of the block, a comparison between numerical and analytical free vibrations is shown with reference to the experimental test performed by Sorrentino et al. (2011) on a masonry wall made of tuff units (Fig. 4). The block is characterized by a height equal to 800 mm and a thickness equal to 123 mm. The figure shows the trend of the ratio of the rotation to the angle of slenderness with respect to time: the dotted grey line relates to the experimental outcomes, the black dotted refers to the analytical solution found by Sorrentino et al. (2011), while the continuous grey line corresponds to the integration procedure used in this paper. The good agreement between the two analytical solutions shows the adequacy of the proposed integration method that allows estimating the force reduction factor as:

$$q = \frac{C \cdot \text{PGA}}{a_{RM}} \quad (10)$$

4 Parametric analyses

Parametric analyses are performed in order to identify the meaningful parameters of the rocking behaviour and consequently the force reduction factor q of the masonry wall. The analyses involve the geometrical aspects and the seismic signal features, as well as the type of kinematic mechanism (two or one sided rocking). Different wall geometries are

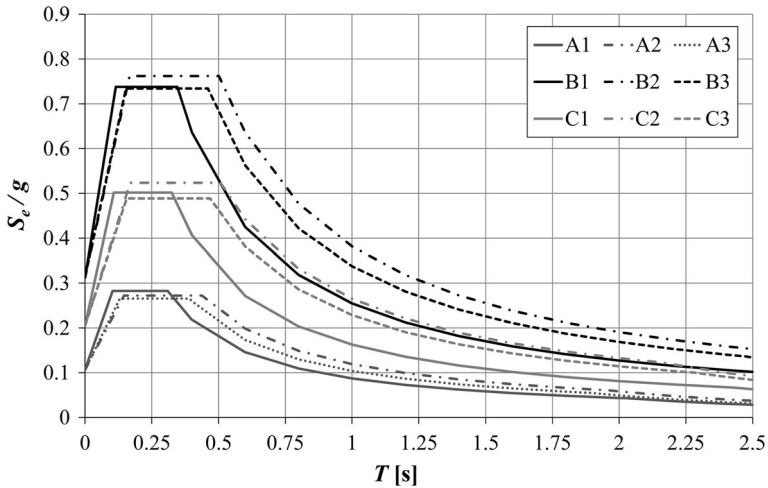


Fig. 5 Elastic response spectra used to generate the acceleration time-histories

considered, varying the height H (from 3 to 11 m) and the angle of slenderness α of the block (3.1° , 6.8° , 11.3°).

For each geometry, incremental dynamic analyses are made with different artificial spectrum-compatible motions, in order to have a sufficient variety of earthquake characteristics. Nine acceleration response spectra, pooled in three groups (A , B and C) characterized by the same peak ground acceleration value (0.106, 0.312 and 0.205 g, respectively), are used to define artificial spectrum-compatible time histories (Fig. 5). For each response spectrum, seven accelerograms are generated according to the code provisions (CEN 2005).

4.1 The response of the two sided model

The first investigated mechanism is the two sided model. In order to evaluate the influence of the energy dissipation model, the force reduction factor is evaluated with Housner's theoretical and Sorrentino's experimental coefficients of restitution r , given by Eqs. (4) and (5), respectively. The force reduction factor is evaluated as the average of the values obtained by the incremental dynamic analyses made with each group composed by seven artificial compatible accelerograms (CEN 2005).

For sake of brevity, the obtained results are reported in terms of q -factor versus the height H of the block for the theoretical (Fig. 6) and experimental (Fig. 7) coefficients of restitution, exclusively for the accelerograms belonging to group B.

For both energy dissipation models, the strength reduction factor increases with increasing slenderness or height of the block. An increment of the slenderness angle, for equal height of the block, corresponds to a stockier element, more stable against the overturning condition. The increase of the strength reduction factor with the height of the block is instead related to the previously described scale effect existing in the model.

Figure 8 shows a comparison of the force reduction factors obtained with the two formulations of the coefficient r for all the considered acceleration time histories. The theoretical one gives always results on the safe side, due to its lower dissipative capacity.

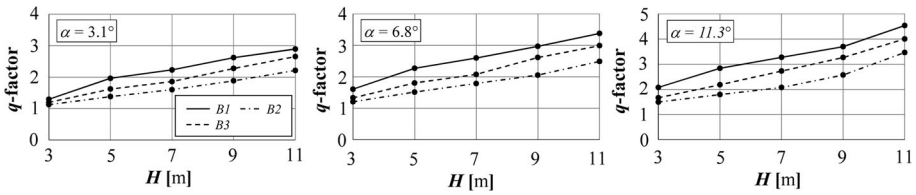


Fig. 6 *q*-factor versus the height *H* of the block for the theoretical coefficients of restitution for the two sided mechanism and for the accelerograms of group *B*; dependence on the angle of slenderness α

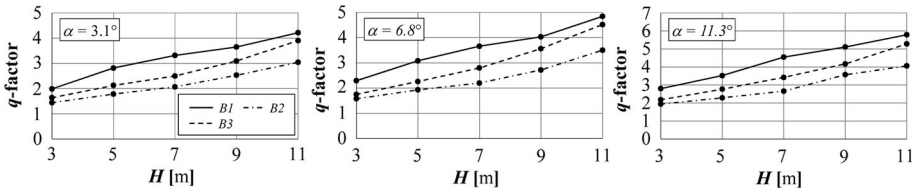
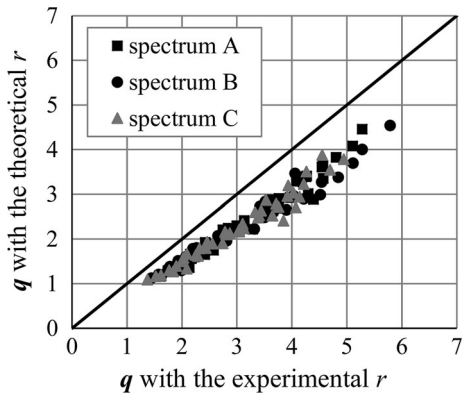


Fig. 7 *q*-factor versus the height *H* of the block for the experimental coefficients of restitution for the two sided mechanism and for the accelerograms of group *B*; dependence on the angle of slenderness α

Fig. 8 Comparison of the force reduction factors obtained with the theoretical and the experimental coefficient of restitution for the two sided mechanism



The collapse condition is in fact reached with a lower value of the seismic acceleration. For this reason, the theoretical coefficient *r* will be only used in the following.

In order to understand the influence of the characteristics of the seismic motion on the dynamic capacity of the rigid block, the *q*-factor of the elements having the intermediate slenderness value $\alpha = 6.8^\circ$ is reported in Fig. 9 for all the chosen response spectra. The outcomes of the incremental analyses confirm the increase of the strength reduction factor with the height *H* and highlight that the *PGA* is not the unique signal characteristic that influences the overturning of the element. Similar results are obtained for the other considered geometries. Even if the *PGA* is the seismic characteristic most widely used to describe an earthquake, it is well known that it does not permit to evaluate the effective destructiveness potential of the seismic event. In many cases, very strong earthquakes do not cause appreciable structural damage, on the contrary, ground motions characterized by lower value of *PGA* have proven to be unexpectedly destructive. Sorrentino et al. (2006), analysing the response of the element to different natural accelerograms, find that the only

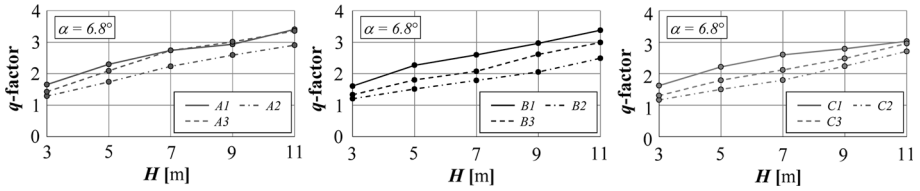


Fig. 9 *q*-factor versus the height *H* of the block with slenderness $\alpha = 6.8$ for the theoretical coefficients of restitution for the accelerograms of group *A*, *B* and *C* for the two sided mechanism

values of the frequency or amplitude are not sufficient for the assessment of the block overturning, while a most representative measure of the seismic motion that causes the overturning of the block is instead the peak ground velocity (*PGV*).

In this paper, in order to introduce a dependency of the force reduction factor on the characteristics of the seismic motion, the Housner Spectrum Intensity (*SI*) is used (Housner 1952). This parameter describes an artificial time history through the area included under the pseudo-velocity response spectrum ($S_v(T)$) in the range between 0.1 and 2.5 s:

$$SI = \int_{0.1s}^{2.5s} S_v(T) dT \tag{11}$$

where *T* is the period of the structure. The values of the Housner Spectrum Intensity of each elastic response spectrum are reported in Table 1.

The outcomes of the performed incremental dynamic analyses are shown introducing a dimensionless coefficient defined as the ratio between the force reduction factor multiplied for the gravitational acceleration and the peak ground acceleration, in the following called effective force reduction factor:

$$q_{eff} = \frac{q \cdot g}{a_g \cdot S} \tag{12}$$

Figures 10, 11 and 12 show the trend of the effective force reduction factor versus the Housner Spectrum Intensity. The mean value of the seven effective force reduction factors is represented in the graphs by dots. The obtained results show as q_{eff} decreases with increasing Housner Spectrum Intensity according to a clear power function law (dotted line in the same figures). It should be noted that a dependence of the response on the pseudo-velocity response spectrum has also been found by other authors (Sorrentino and Masiani

Table 1 Values of the Housner Spectrum Intensity

Group	PGA (g)	Spectrum	SI (cm)
A	0.106	A1	31.18
		A2	41.04
		A3	35.92
B	0.312	B1	92.05
		B2	133.45
		B3	119.06
C	0.205	C1	59.05
		C2	91.69
		C3	80.24

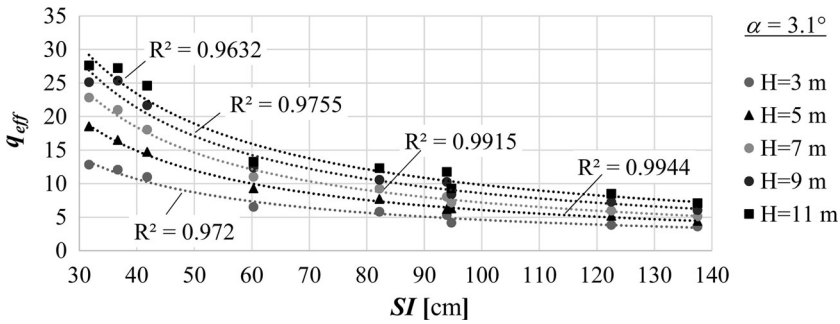


Fig. 10 q_{eff} versus SI for the two sided mechanism, for the block with slenderness $\alpha = 3.1^\circ$

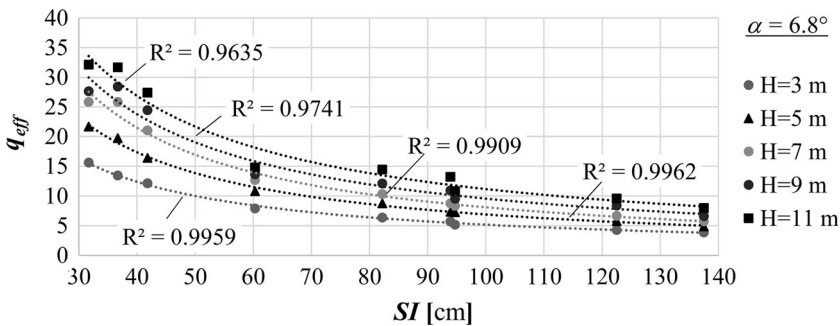


Fig. 11 q_{eff} versus SI for the two sided mechanism, for the block with slenderness $\alpha = 6.8^\circ$

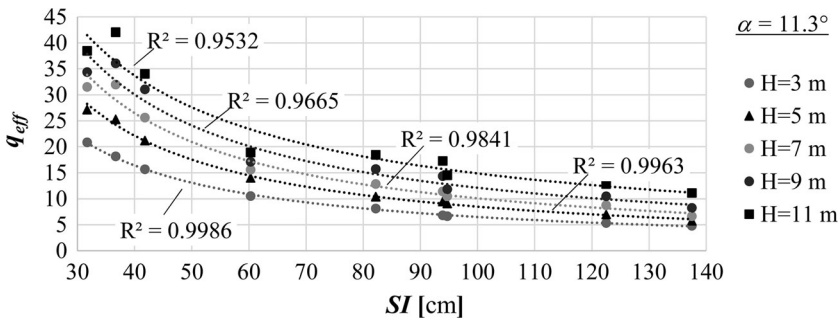


Fig. 12 q_{eff} versus SI for the two sided mechanism, for the block with slenderness $\alpha = 11.3^\circ$

2007; Giresini et al. 2015). The determination coefficients R^2 of the statistical regressions are also reported in the figures.

4.2 The response of the one sided model

In this section the one sided rocking model is investigated and the force reduction factor is evaluated. The two different energy dissipation models (Eqs. 6 and 7) suggested by Sorrentino et al. (2011) are taken into account. Similarly to the previous section, the q -factor versus the slenderness α is plotted exclusively for the accelerograms belonging to the group

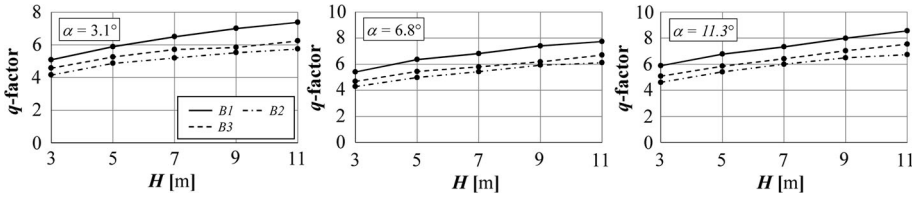


Fig. 13 *q*-factor versus the height *H* of the block for the theoretical coefficients of restitution for the one sided mechanism and for the accelerograms of group *B*; dependence on the angle of slenderness α

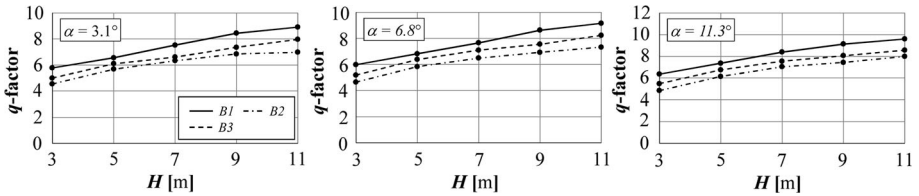
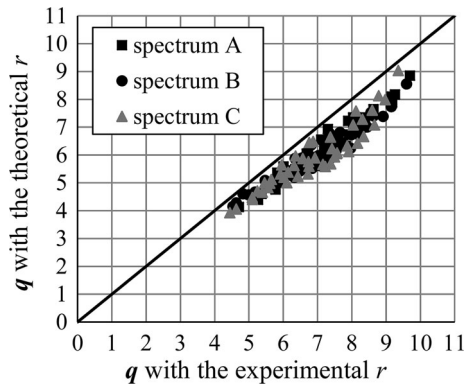


Fig. 14 *q*-factor versus the height *H* of the block for the experimental coefficients of restitution for the one sided mechanism and for the accelerograms of group *B*; dependence on the angle of slenderness α

Fig. 15 Comparison of the force reduction factors obtained with the theoretical and the experimental coefficient of restitution for the one sided mechanism



B (Figs. 13, 14). Also in this mechanism, the *q*-factor increases with increasing slenderness or height of the block and the overturning of the element is not only influenced by the *PGA*. Similar results are found for the other geometries and seismic inputs.

The theoretical results are shown to be again on the safe side (Fig. 15), hence only the theoretical coefficient *r* is used in the following to study the dependence of the *q*-factor on the Housner Spectrum Intensity.

Similarly to the previous case, the effective force reduction factor decreases with increasing Housner Spectrum Intensity, according to a power function law (Figs. 16, 17, 18).

4.3 Trilinear moment-rotation law

This section is devoted to the assessment of the force reduction factor by using a trilinear moment-rotation law, in order to highlight the differences with the classic approach when a deviation of the actual geometry of the wall from the perfectly parallelepiped one occurs

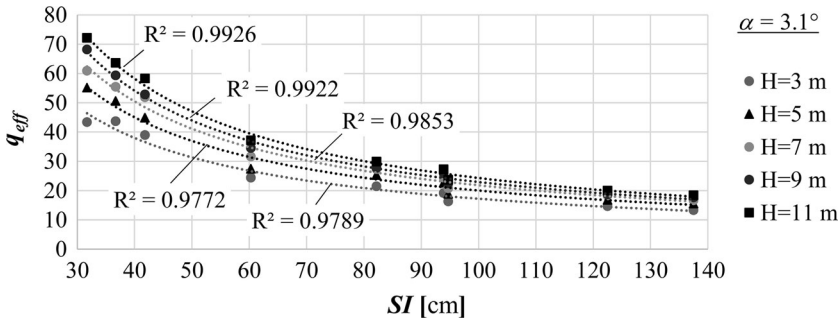


Fig. 16 q_{eff} versus SI for the one sided mechanism, for the block with $\alpha = 3.1^\circ$

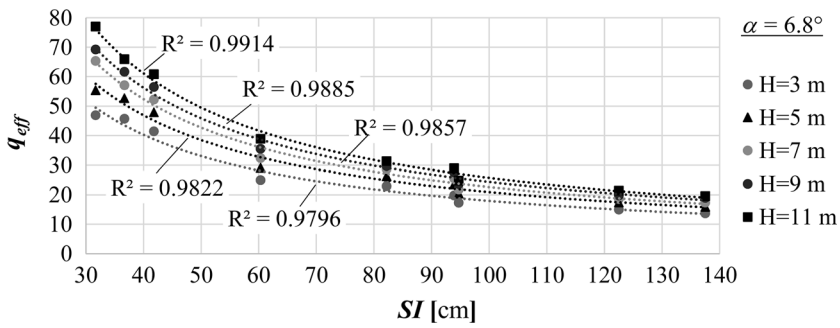


Fig. 17 q_{eff} versus SI for the one sided mechanism, for the block with $\alpha = 6.8^\circ$

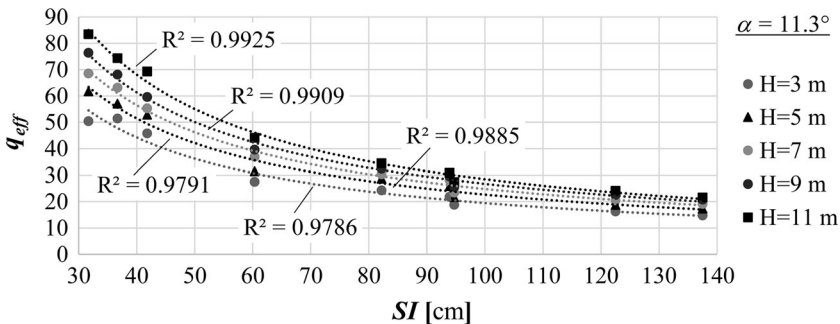


Fig. 18 q_{eff} versus SI for the one sided mechanism, for the block with $\alpha = 11.3^\circ$

(Al Shawa et al. 2015). The values of the parameters defining the considered rocking block model can be set on the basis of experimental tests. In this paper, Δ_1 is set equal to 0.06 and 0.02 according to Doherty et al. (2002) and Al Shawa et al. (2015) respectively. Regarding to the parameter Δ_2 , both authors suggest using a value equal to 0.28.

Figure 19 shows a comparison of the force reduction factors obtained with the two approaches for an intermediate geometry of the block, characterized by a slenderness angle and a height equal to 6.8° and 7 m respectively. All the nine acceleration response spectra belonging to the groups A, B and C have been considered. The q -factors obtained according

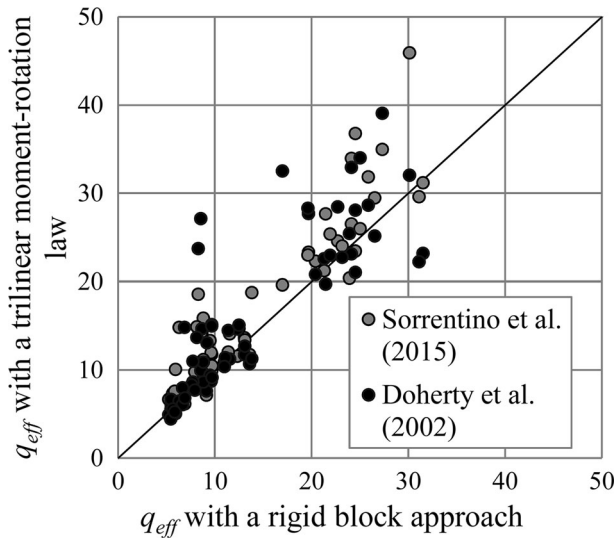


Fig. 19 Influence of the trilinear simplified moment-rotation law for the block with $\alpha = 6.8^\circ$ and $H = 7$ m

to the classic rigid body approach and to the trilinear model are indicated on the x -axis and y -axis, respectively. The black colour is used to identify the results obtained with the values of the parameters suggested by Doherty et al. (2002), while the ones obtained according to Al Shawa et al. (2015) are plotted in grey. It is found that the percentage of conservative cases increases adopting a trilinear moment-rotation law for both considered values of the parameters Δ_1 and Δ_2 as in Al Shawa et al. (2015).

5 Analytical formulations for evaluating the Q -factor

In this section, starting from the results of the performed numerical analyses, analytical formulations for evaluating the force reduction factor are proposed for both the considered mechanisms. Since the performed dynamic analyses consider non-load carrying elements, the proposed relationships can be used only for masonry walls not supporting any upper horizontal structure.

As previously stated, the general formulation of the effective force reduction factor assumes the form:

$$q_{eff} = C_1 S I^{C_2} \quad (13)$$

where the parameters C_1 and C_2 are function of the geometrical characteristics H and α of the block. For both the investigated models, constant values can be assumed for the coefficient C_2 , because of its low variability. In particular, the range of C_2 is $[-0.919; -1.07]$ for the two sided mechanism and $[-0.862; -0.95]$ for the one sided, assuming SI in cm. For this reason, values equal to -1.0 and -0.9 are respectively used for the two formulations.

Concerning C_1 , for both the two mechanisms, a linear dependence on H and α is assumed:

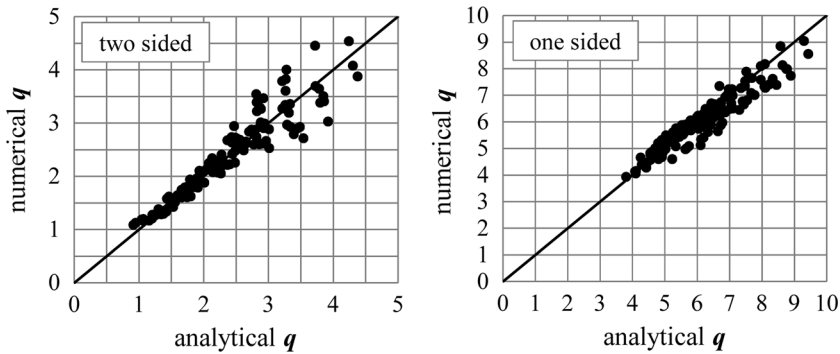


Fig. 20 Comparison between the q -factor obtained from the numerical procedure and from the analytical proposed formulation

$$C_1 = A_1\alpha + A_2H + A_3 \tag{14}$$

in which the coefficients A_1 , A_2 and A_3 are obtained for each model through a regression of the numerical outcomes with the ordinary least squares method.

The following novel relationships for the evaluation of the q -factor are drawn by applying the above procedure:

$$q_{\text{two_sided}} = q_{\text{eff}} \frac{a_g \cdot S}{g} = (30 \cdot \alpha + 78 \cdot H + 90) \cdot SI^{-1.0} \tag{15}$$

$$q_{\text{one_sided}} = q_{\text{eff}} \frac{a_g \cdot S}{g} = (23 \cdot \alpha + 65 \cdot H + 840) \cdot SI^{-0.9} \tag{16}$$

with α in degree, H in m and SI in cm.

The effectiveness of these analytical laws is highlighted in Fig. 20 in which the numerical force reduction factor is plotted versus the analytical one for the two examined models.

5.1 Comparison with the analysis performed with natural records

In order to confirm the observed trends of the effective force reduction factor with the Housner Spectrum Intensity in the case of use of spectrum-compatible time histories, further analyses are performed considering the natural records summarized in Table 2 together with the main seismic characteristics.

With reference to the intermediate geometry of the block, characterized by a slenderness angle and a height to 6.8° and 7 m respectively, the effective force reduction factors for both two sided and one sided mechanisms have been evaluated.

Figure 21 shows the obtained results for the considered geometry of the block and the case of the two sided mechanism. The trend of the effective force reduction factor with the Housner Spectrum Intensity evaluated according to the proposed formulation (Eq. 15) is plotted with a continuous black line; the effective force reduction factors assessed imposing to the block the time histories of Table 2 are superimposed by means of black points. The same figure shows the effectiveness of the proposed analytical formulation: the

Table 2 Seismic characteristics of the considered natural records

ID	Event	Date	Mw	PGA (g)	PGV (cm/s)	PGD (cm)	Δt (s)	SI (cm)
TH1	L'Aquila	2009-IV-06	6.3	0.03	1.8	0.6	118.995	9.04
TH2	South Iceland	2000-VI-21	6.4	0.02	4.29	2.46	62.99	9.81
TH3	Irpinia	1980-XI-23	6.9	0.06	5.06	2.01	66.48	20
TH4	Irpinia	1980-XI-23	6.9	0.06	6.28	2.57	66.48	21.92
TH5	Campano Lucano	1980-XI-23	6.9	0.06	5.89	5.01	66.51	23.56
TH6	Friuli	1976-IX-15	6	0.16	9.98	2.14	72.47	25.23
TH7	Umbria-Marche	1997-IX-26	6	0.07	8.95	1.79	50.495	30.59
TH8	Bingol	2003-V-01	6.3	0.3	20.97	3.73	64.71	74.53
TH9	Irpinia	1980-XI-23	6.9	0.16	26.02	9.68	85.995	113.42
TH10	Imperial Valley	1940-V-19	7	0.32	29.8	13.3	53.8	124.27
TH11	L'Aquila	2009-IV-06	6.3	0.33	32.14	7.19	100	137.5

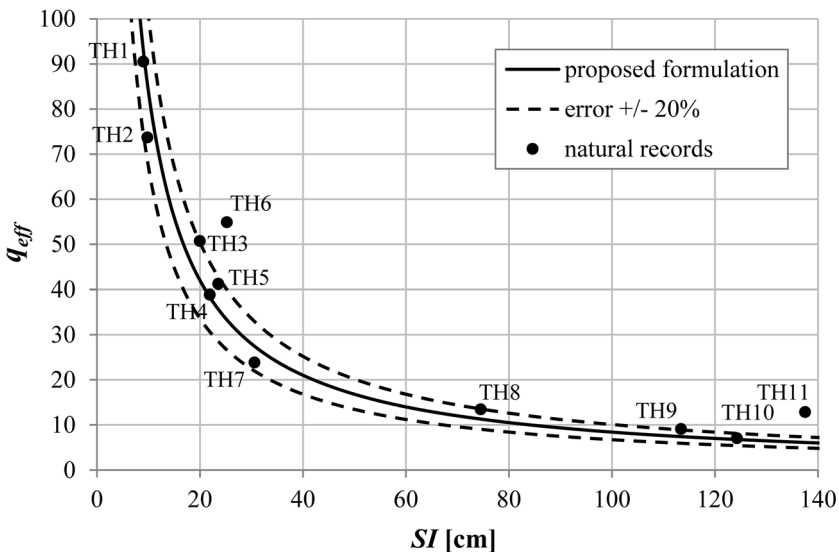


Fig. 21 q_{eff} evaluated with natural records for the two sided mechanism for the block with $\alpha = 6.8^\circ$ and $H = 7$ m

obtained results, evaluated with natural records, are in fact included within an error zone equal to $\pm 20\%$ of the proposed law -superimposed with a black dashed line—and only in few cases this interval has been exceeded.

Similarly to the previous case, Fig. 22 shows the results obtained considering the same geometry of the block, for the case of the one sided mechanism. A good agreement between the effective force reduction factors evaluated using natural records and the formulation of Eq. (16) is found, also confirming the effectiveness of the proposed law for the one sided mechanism.

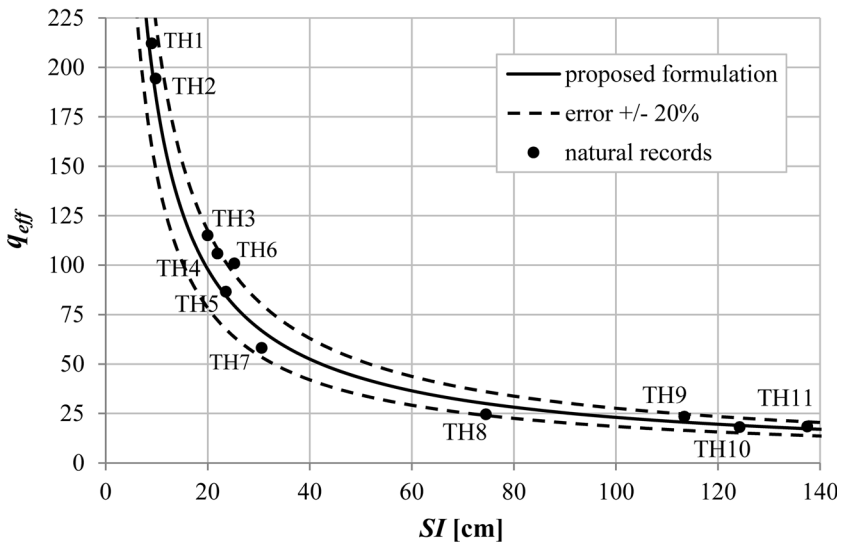


Fig. 22 q_{eff} evaluated with natural records for the one sided mechanism for the block with $\alpha = 6.8^\circ$ and $H = 7$ m

6 Conclusions

In this paper, the out-of-plane response of masonry elements is analytically investigated in the framework of the dynamic equation of motion of the rigid body, according to the material hypothesis of infinite strength and stiffness in compression and tensile strength equal to zero.

Two local collapse mechanisms, the two sided and the one sided rocking, have been here examined, with the aim to properly evaluate the corresponding force reduction factor. This last is defined as the ratio between the seismic acceleration value causing the collapse of the masonry element and the one corresponding to the activation of the rocking motion. The influence of considering a simplified trilinear moment-rotation law in the assessment of the rocking behavior of the masonry block is also discussed.

Parametric analyses have been performed, numerically solving the dynamic equation of motion with increasing magnitude of the seismic action until the attainment of the collapse condition of the block. The main parameters of the model have been varied in order to evaluate their impact on the global response of the system: the geometrical characteristics of the block, i.e. the height and the angle of slenderness; the energy dissipation model, describing the dissipative phenomena occurring when the block undergoes an impact to the base; the main features of the seismic input.

It is shown that the theoretical dissipation models lead always to results on the safe side with respect to the experimental ones, due to their lower dissipative capacity. The collapse condition is in fact reached with a lower value of the seismic acceleration.

It is worth highlighting that the response of the block does not depend only on the value of the peak ground acceleration: other characteristics of the seismic signal have to be taken into account to effectively catch the collapse behaviour. It is furthermore shown that a power function law exists between an effective force reduction factor, defined as the ratio

of the force reduction factor to the maximum value of the acceleration time history, and the Housner Spectrum Intensity, for both the two examined models.

Eventually, novel formulations for evaluating the force reduction factor of the two rocking models, dependent on the geometrical characteristics of the block and on the Housner Spectrum Intensity, have been here proposed. Their effectiveness has been also shown considering the implementation of both spectrum-compatible accelerograms and natural records.

References

- Al Shawa O, Liberatore D, Sorrentino L (2015) Valutazione Normativa della Sicurezza per Meccanismi Locali di Collasso di Pareti Murarie. 16 Convegno Anidid “L’ingegneria sismica in Italia”. L’Aquila 13–17 settembre, paper 2225
- CEN (2005) EN 1998–1:2005, Eurocode 8: “design of structures for earthquake resistance - Part 1: general rules, seismic actions and rules for buildings”. Brussels
- CMIT (Circolare Ministero Infrastrutture) (2009) Circolare 2 febbraio 2009 n. 617 Istruzioni per l’applicazione delle “Nuove norme tecniche per le costruzioni” di cui al DM 14 gennaio 2008. Gazzetta Ufficiale della Repubblica Italiana n. 47, Supplemento Ordinario n. 27
- Coccia S, Como M (2015) Minimum thrust of rounded cross vaults. *Int J Archit Herit Conserv Anal Restor* 9(4):468–484. doi:[10.1080/15583058.2013.804965](https://doi.org/10.1080/15583058.2013.804965)
- Coccia S, Como M, Di Carlo F (2015a) Wind strength of gothic cathedrals. *Eng Fail Anal* 55:1–25. doi:[10.1016/j.engfailanal.2015.04.019](https://doi.org/10.1016/j.engfailanal.2015.04.019)
- Coccia S, Di Carlo F, Rinaldi Z (2015b) Collapse displacements for a mechanism of spreading-induced supports in a masonry arch. *Int J Adv Struct Eng* 7(3):307–320. doi:[10.1007/s40091-015-0101-x](https://doi.org/10.1007/s40091-015-0101-x)
- Coccia S, Di Carlo F, Imperatore S (2016) Strength reduction factor for out-of-plane failure mechanisms of masonry walls. In: 16th international brick and block masonry conference, June 26–30, Padova, Italy
- Costa AA, Arède A, Penna A, Costa A (2012) Experimental evaluation of the coefficient of restitution of rocking stone masonry façades. In: 15th international brick and block masonry conference
- Costa AA, Arède A, Penna A, Costa A (2013) Free rocking response of a regular stone masonry wall with equivalent block approach: experimental and analytical evaluation. *Earthq Eng Struct Dyn* 42:2297–2319. doi:[10.1002/eqe.2327](https://doi.org/10.1002/eqe.2327)
- D’Ayala D, Shi Y (2011) Modeling masonry historic buildings by multi-body dynamics. *Int J Archit Herit* 5:483–512. doi:[10.1080/15583058.2011.557138](https://doi.org/10.1080/15583058.2011.557138)
- D’Ayala DF, Paganoni S (2011) Assessment and analysis of damage in L’Aquila historic city centre after 6th April 2009. *Bull Earthq Eng* 9(1):81–104. doi:[10.1007/s10518-010-9224-4](https://doi.org/10.1007/s10518-010-9224-4)
- D’Ayala D, Speranza E (2003) Definition of collapse mechanisms and seismic vulnerability of historic masonry buildings. *Earthq Spectra* 19(3):479–509. doi:[10.1193/1.1599896](https://doi.org/10.1193/1.1599896)
- D’Ayala D, Spence R, Oliveira C, Pomonis A (1997) Earthquake loss estimation for Europe’s historic town centres. *Earthq Spectra* 13(4):773–793
- De Felice G (2011) Out-of-plane seismic capacity of masonry depending on wall section morphology. *Int J Archit Herit* 5(4–5):466–482. doi:[10.1080/15583058.2010.530339](https://doi.org/10.1080/15583058.2010.530339)
- De Lorenzis L, DeJong M, Ochsendorf J (2007) Failure of masonry arches under impulse base motion. *Earthq Eng Struct Dyn* 36(14):2119–2136. doi:[10.1002/eqe.719](https://doi.org/10.1002/eqe.719)
- Doherty K, Griffith MC, Lam N, Wilson J (2002) Displacement-based seismic analysis for out-of-plane bending of unreinforced masonry walls. *Earthq Eng Struct Dyn* 31(4):833–850. doi:[10.1002/eqe.126](https://doi.org/10.1002/eqe.126)
- Ferreira TM, Costa AA, Vicente R, Varum H (2015) A simplified four-branch model for the analytical study of the out-of-plane performance of regular stone URM walls. *Eng Struct* 83:140–153. doi:[10.1016/j.engstruct.2014.10.048](https://doi.org/10.1016/j.engstruct.2014.10.048)
- Giresini L, Fragiaco M, Lourenço PB (2015) Comparison between rocking analysis and kinematic analysis for the dynamic out-of-plane behavior of masonry walls. *Earthq Eng Struct Dyn* 44:2359–2376. doi:[10.1002/eqe.2592](https://doi.org/10.1002/eqe.2592)
- Hao H, Zhou Y (2011) Rigid structure response analysis to seismic and blast induced ground motions. *Proced Eng* 14:946–955. doi:[10.1016/j.proeng.2011.07.119](https://doi.org/10.1016/j.proeng.2011.07.119)
- Hogan SJ (1992) On the motion of a rigid block, tethered at one corner, under harmonic forcing. *Proc R Soc Math Phys Sci* 439(1905):35–45. doi:[10.1098/rspa.1992.0132](https://doi.org/10.1098/rspa.1992.0132)

- Housner GW (1952) Intensity of ground motion during strong earthquakes. California Inst of Tech Pasadena Earthquake Engineering Research Lab, California
- Housner GW (1963) The behavior of inverted pendulum structures during earthquakes. *Bull Seismol Soc Am* 53(2):403–417
- Kounadis AN (2010) On the dynamic overturning instability of a rectangular rigid block under ground excitation. *Open Mech J* 4:43–57. doi:[10.2174/18741584010040100043](https://doi.org/10.2174/18741584010040100043)
- Makris N, Konstantinidis D (2003) The rocking spectrum and the limitations of practical design methodologies. *Earthq Eng Struct Dyn* 32(2):265–289. doi:[10.1002/eqe.223](https://doi.org/10.1002/eqe.223)
- Papantonopoulos C, Psycharis IN, Papastamatiou DY, Lemos JV, Mouzakis HP (2002) Numerical prediction of the earthquake response of classical columns using the distinct element method. *Earthq Eng Struct Dyn* 31:1699–1717. doi:[10.1002/eqe.185](https://doi.org/10.1002/eqe.185)
- Peña F, Prieto F, Lourenço PB, Campos Costa A, Lemos JV (2007) On the dynamics of rocking motion of single rigid-block structures. *Earthq Eng Struct Dyn* 36:2383–2399. doi:[10.1002/eqe.739](https://doi.org/10.1002/eqe.739)
- Prieto F, Lourenço PB (2005) On the rocking behavior of rigid objects. *Meccanica* 40(2):121–133. doi:[10.1007/s11012-005-5875-7](https://doi.org/10.1007/s11012-005-5875-7)
- Shawa OA, de Felice G, Mauro A, Sorrentino L (2012) Out-of-plane seismic behaviour of rocking masonry walls. *Earthq Eng Struct Dyn* 41:949–968. doi:[10.1002/eqe.1168](https://doi.org/10.1002/eqe.1168)
- Sorrentino L, Masiani R (2007) Risposta fuori del piano di pareti murarie, libere e vincolate in sommità, a segnali naturali. 12 Convegno Nazionale “L’Ingegneria Sismica in Italia”, Pisa 10-14.-06.2007, paper 124
- Sorrentino L, Masiani R, Decanini LD (2006) Overturning of rocking rigid bodies under transient ground motions. *Struct Eng Mech* 22(3):293–310. doi:[10.12989/sem.2006.22.3.293](https://doi.org/10.12989/sem.2006.22.3.293)
- Sorrentino L, Kunnath S, Monti G, Scalora G (2008a) Seismically induced one-sided rocking response of unreinforced masonry façades. *Eng Struct* 30(8):2140–2153. doi:[10.1016/j.engstruct.2007.02.021](https://doi.org/10.1016/j.engstruct.2007.02.021)
- Sorrentino L, Masiani R, Griffith MC (2008b) The vertical spanning strip wall as a coupled rocking rigid body assembly. *Struct Eng Mech* 29(4):433–453. doi:[10.12989/sem.2008.29.4.433](https://doi.org/10.12989/sem.2008.29.4.433)
- Sorrentino L, Al Shawa O, Decanini LD (2011) The relevance of energy damping in unreinforced masonry rocking mechanisms. *Exp Anal Investig Bull Earthq Eng* 9(5):1617–1642. doi:[10.1007/s10518-011-9291-1](https://doi.org/10.1007/s10518-011-9291-1)
- Yim CS, Chopra AK, Penzien J (1980) Rocking response of rigid blocks to earthquakes. *Earthq Eng Struct Dyn* 8(6):565–587. doi:[10.1002/eqe.4290080606](https://doi.org/10.1002/eqe.4290080606)
- Zhang J, Makris N (2001) Rocking response of free-standing blocks under cycloidal pulses. *J Eng Mech* 127(5):473–483. doi:[10.1061/\(ASCE\)0733-9399\(2001\)127:5\(473\)](https://doi.org/10.1061/(ASCE)0733-9399(2001)127:5(473))